

Photodisintegration of the triton with realistic potentials

W. Schadow and W. Sandhas

Physikalisches Institut der Universität Bonn

Endenicher Allee 11-13

53115 Bonn, Germany

Abstract

The process $\gamma + t \rightarrow n + d$ is treated by means of three-body integral equations employing in their kernel the W-Matrix representation of the subsystem amplitudes. As compared to the plane wave (Born) approximation the full solution of the integral equations, which takes into account the final state interaction, shows at low energies a 24% enhancement. The calculations are based on the semirealistic Malfliet-Tjon and the realistic Paris and Bonn B potentials. For comparison with earlier calculations we also present results for the Yamaguchi potential. In the low-energy region a remarkable potential dependence is observed, which vanishes at higher energies.

21.45.+v, 25.10.+s, 25.20.-x, 27.10.+h

Typeset using REVTeX

I. INTRODUCTION

The photodisintegration of ${}^3\text{H}$ and ${}^3\text{He}$ and the inverse reaction, the radiative capture of protons or neutrons by deuterons, have been intensively investigated in the past. Due to the fact that the corresponding matrix elements contain both the three-body bound and continuum states, these reactions are expected to be a good testing ground for the underlying two-body potential. In early calculations by Barbour and Phillips [1] it has been shown that an exact treatment of the continuum states results in a considerable enhancement of the cross section in the peak region. In that work and in the following by Gibson and Lehman [2] only simple s -wave interactions of Yamaguchi type have been used, while d -components ($j \leq 1^+$) were incorporated in [3]. The role of p -wave contributions in the two-body input with respect to the three-body cross section was investigated by Fonseca and Lehman [4], using again Yamaguchi terms in the interaction. More recently, calculations based on separable representations of the Bonn A and Paris potentials, including their higher partial wave contributions, were performed for polarization observables at some specific energies [5–8].

In the present work we calculate the differential cross sections at 90° for the Yamaguchi, Malfliet-Tjon, Paris, and Bonn B potentials over an energy region from threshold up to 40 MeV. The potential dependence, the effect of higher partial waves, and the role of meson exchange currents, taken into account via Siegert’s theorem, are investigated.

Technically the calculations are based on the Faddeev-type Alt-Grassberger-Sandhas (AGS) formalism [9] adjusted to photonuclear processes [10], as done already in [2]. The separable representation of the subsystem T matrices, relevant in this context, is chosen according to the W -Matrix approach [11]. This approximation combines high accuracy with considerable simplicity [12].

A more reliable, still fairly simple representation of the two-body input is provided by the Ernst-Shakin-Thaler method [13]. Calculations employing the corresponding PEST, BEST, and NEST potentials [14–16] will be presented in a subsequent publication.

II. FORMALISM

The Alt-Grassberger-Sandhas (AGS) equations are well known to go over into effective two-body Lippmann-Schwinger equations [9] when representing the input two-body T -operators in separable form. The neutron-deuteron off-shell scattering amplitude $\mathcal{T}(\vec{q}, \vec{q}'')$, thus, is determined by

$$\mathcal{T}(\vec{q}, \vec{q}'') = \mathcal{V}(\vec{q}, \vec{q}'') + \int d^3 q' \mathcal{V}(\vec{q}, \vec{q}') \mathcal{G}_0(\vec{q}') \mathcal{T}(\vec{q}', \vec{q}''). \quad (1)$$

Applying the same technique to the photodisintegration of the triton into neutron and deuteron, i.e. to the process $\gamma + t \rightarrow n + d$, an integral equation of rather similar structure is obtained [1,2,10],

$$\mathcal{M}(\vec{q}) = \mathcal{B}(\vec{q}) + \int d^3 q' \mathcal{V}(\vec{q}, \vec{q}') \mathcal{G}_0(\vec{q}') \mathcal{M}(\vec{q}'), \quad (2)$$

where $\mathcal{M}(\vec{q})$ represents an off-shell extension of the full photodisintegration amplitude

$$M(\vec{q}) = {}^{(-)}\langle \vec{q}; \psi_d | H_{\text{em}} | \Psi_t \rangle. \quad (3)$$

In both these equations the kernel is given by the effective neutron-deuteron potential \mathcal{V} and the corresponding effective free Green function \mathcal{G}_0 defined in Ref. [9]. However, in Eq. (2) the inhomogeneity of Eq. (1) is replaced by an off-shell extension $\mathcal{B}(\vec{q})$ of the plane-wave (Born) amplitude

$$B(\vec{q}) = \langle \vec{q} | \langle \psi_d | H_{\text{em}} | \Psi_t \rangle. \quad (4)$$

Here $|\Psi_t\rangle$ and $|\psi_d\rangle$ denote the triton and deuteron states, $|\vec{q}\rangle$ the momentum state of the neutron relative to the center of mass of the deuteron, and H_{em} the electromagnetic operator. Thus, by this replacement any working program for $n-d$ scattering can immediately be applied to the above photoprocess.

The results presented in this paper are, in fact, obtained by extending recent $n-d$ calculations [12,17] in this manner. As in these references, the separable part of the W -matrix representation [11] of the two-body T matrices is employed,

$$T_{ll'}^\eta(p, p', E + i0) = \sum_{\hat{l}\hat{l}'} p^l W_{l\hat{l}}^\eta(p, k; E) \Delta_{\hat{l}\hat{l}'}^\eta(E + i0) W_{l'\hat{l}'}^\eta(p', k; E) p'^{l'} . \quad (5)$$

Here l and l' are the orbital angular momenta, and $\eta = (s, j; i)$ stands for the spin, the angular momentum j [with the coupling sequence $(l, s)j$] and the isospin i of the two-body subsystem. With the form factors $W_{l\hat{l}}^\eta$ and the propagators $\Delta_{\hat{l}\hat{l}'}^\eta$ of this representation Eq. (2) reads, after partial wave decomposition and antisymmetrization,

$${}^\Gamma \mathcal{M}_{\hat{l}}^b(q, E) = {}^\Gamma \mathcal{B}_{\hat{l}}^b(q, E) + \sum_{b'\hat{l}', \hat{l}''} \int_0^\infty dq' q'^2 {}^\Gamma \mathcal{V}_{\hat{l}\hat{l}'}^{bb'}(q', E) \Delta_{\hat{l}\hat{l}'}^{\eta'}(E - \frac{3}{4} q'^2) {}^\Gamma \mathcal{M}_{\hat{l}''}^{b'}(q', E) \quad (6)$$

and its inhomogeneity is given by

$${}^\Gamma \mathcal{B}_{\hat{l}}^b(q, E) = \sqrt{3} \sum_l \int_0^\infty dp p^{l+2} \langle p q b l \Gamma I | W_{l\hat{l}}^\eta(k, p, E - \frac{3}{4} q^2) G_0(E + i0) H_{\text{em}} | \Psi_t \rangle . \quad (7)$$

Here, G_0 and $\langle p q b l \Gamma I |$ represent the free three-body Green function and the partial wave projection of the three-body plane wave state $\langle \vec{q} | \langle \vec{p} |$. The detailed structure of the effective potential ${}^\Gamma \mathcal{V}_{\hat{l}\hat{l}'}^{bb'}$ can be found in Ref. [12]. The label b denotes the set $(\eta K L)$ of quantum numbers, where K and L are the channel spin of the three nucleons [with the coupling sequence $(j, \frac{1}{2})K$] and the relative angular momentum between the two-body subsystem and the third particle, respectively. Γ is the total angular momentum following from the coupling sequence $(K, L)\Gamma$, and I is the total isospin.

The Born amplitude contains the triton bound state $|\Psi_t\rangle$, which may be calculated by any of the various bound-state methods. Consistently with the present approach we employ for this purpose the partial wave projected homogeneous version of Eq. (1),

$$F_{\hat{l}}^b(q) = \sum_{b'\hat{l}'l} \int_0^\infty dq' q'^2 \mathcal{V}_{\hat{l}\hat{l}'}^{bb'}(q, q', E_T) \Delta_{\hat{l}\hat{l}'}^{\eta}(E_T - \frac{3}{4} q'^2) F_{\hat{l}'}^{b'}(q') . \quad (8)$$

Its solutions, the three-body “form-factors” $F_{\hat{l}}^b(q)$, are related to $|\Psi_t\rangle$ according to [9] by

$$|\Psi_t\rangle = \sum_{\gamma b \hat{l} \hat{l}'} \iint dq dp q^2 p^2 G_0(E_T) |(\gamma) q p b l \Gamma I\rangle W_{l\hat{l}}(p, k, E_T - \frac{3}{4} q^2) \Delta_{\hat{l}\hat{l}'}^{\eta}(E_T - \frac{3}{4} q^2) F_{\hat{l}'}^b(q) . \quad (9)$$

Here, the summation runs over all two-fragment partitions γ , the variables and quantum numbers being understood in the corresponding set of Jacobi coordinates.

The electromagnetic operator entering Eq. (7) is, at the low energies considered, essentially a dipole operator. Ignoring meson-exchange currents it is given by

$$H'_{\text{em}} = \sqrt{\frac{4\pi}{3}} \sum_{i=1}^3 e_i p_i Y_{1\lambda}(\vartheta, \varphi) . \quad (10)$$

With exchange currents it takes, according to Siegert's theorem [18], the form [19]

$$H_{\text{em}} = -i \sqrt{\frac{4\pi}{3}} (E_f - E_t) \sum_{i=1}^3 e_i r_i Y_{1\lambda}(\vartheta, \varphi) . \quad (11)$$

Here E_f and E_t denote the final and the triton energies, r_i the nucleon center-of-mass coordinates, p_i the corresponding momenta, e_i the electric charges, and λ the polarization of the photon.

The on-shell restricted solutions ${}^\Gamma M_l^b$ of the integral Eq. (6) yield the photodisintegration amplitude via the partial-wave summation

$$\begin{aligned} & {}^{(-)} \langle \vec{q} s m_s; \psi_d j m_j | H_{\text{em}} | \Psi_t \Gamma' M_{\Gamma'} \rangle \\ &= \sum_{\Gamma M_{\Gamma} b \hat{l} M_K M_L} \langle j m_j s m_s | K M_K \rangle \langle K M_K L M_L | \Gamma M_{\Gamma} \rangle Y_{L M_L}(\hat{q}) {}^\Gamma M_l^b (q, E_d + \frac{3}{4} q^2) , \end{aligned} \quad (12)$$

where now, in contrast to Eq. (3), the spin and angular momentum quantum numbers of the neutron ($s m_s$), deuteron ($j m_j$), triton ($\Gamma' M_{\Gamma'}$), and the polarization (λ) of the photon are explicitly given. Denoting this amplitude by $M(\vec{q})_{m_s m_j M_{\Gamma'} \lambda}$, the cross section is obtained in the standard way by

$$\frac{d\sigma}{d\Omega} = \frac{2\pi^2}{3} \frac{q}{E_{\gamma} c} \sum_{m_s m_j} \sum_{M_{\Gamma'}, \lambda} \left| M(\vec{q})_{m_s m_j M_{\Gamma'} \lambda} \right|^2 . \quad (13)$$

Here we have averaged over the initial states and summed over the final states.

III. RESULTS

As a first test of our numerical program we performed calculations for the Yamaguchi [21] potential in order to compare them with the corresponding results by Gibson and Lehman [2]. Unfortunately, employing the same sets of parameters as in this reference, we

read off from the analytically given relations somewhat different values for the two-body scattering length, effective range, and deuteron binding energy (Table I). The triton binding energies, obtained by solving the homogeneous three-body equations, differ in one case, the symmetric Tabakin potential, where we found -9.72MeV instead of -9.33MeV (Table III). These discrepancies mean that our photodisintegration results cannot be expected to fully agree with the ones of Ref. [2].

Figure 1 compares our cross sections for triton-photodisintegration (solid line) with the calculations by Gibson and Lehman [2] (dashed line). The disagreement, in particular in the peak region, is reduced when replacing in the Siegert operator our triton energy by the Gibson-Lehman value (short-dashed line). Figure 2 shows the same comparison, but now for the ^3He photodisintegration. Since there is no disagreement between the ^3He binding energies, a correspondingly modified curve does not exist. The remaining discrepancies, therefore, have to be attributed to numerical uncertainties, which are not unexpected in view of the level of accuracy reached in early calculations. Within these limits we consider our results for the Yamaguchi potential consistent with the ones of Ref. [2].

The differential cross sections obtained for the Paris [22], Bonn *B* [23], Malfliet-Tjon (MT I-III) [24], and Yamaguchi potentials are shown in Figure 3. Most remarkable is the strong potential dependence in the peak region, which vanishes at higher energies. A further observation, which should be relevant in model calculations or when going over to higher particle numbers [25], is the proximity of the Paris and Malfliet-Tjon results on the one hand, and less closely the Bonn *B* and Yamaguchi potentials on the other hand.

In Figure 4 we contrast, for the Paris potential, the solution of the integral equation (solid line) with the corresponding plane-wave (Born) approximation (dashed line). It is seen that the full solution is enhanced by about 24% at the peak. A similar enhancement was observed for simpler interactions already in Ref. [1]. The upper curves are the ones based on the Siegert-operator (11), the lower ones correspond to the non-Siegert operator (10). There is a factor of two between the Siegert and non-Siegert results, which demonstrates the relevance of meson-exchange currents. For a detailed discussion of the same phenomenon in

case of deuteron and ^4He photodisintegration we refer to Refs. [20] and [25], respectively.

Figures 5 and 6 compare our cross sections for the s- and d-wave projected Paris and Bonn B potentials with the data from Refs. [26–28]. Figures 7 and 8 show the same with inclusion of the subsystem p waves, which leads to a reduction of the peak by 8–10%. Up to 25 MeV the best agreement with the data is achieved for the Bonn B potential. In view of the experimental errors the relevance of this observation is, of course, somewhat questionable. At higher energies the potential dependence vanishes. It is, however, seen that the incorporation of the p waves is essential for the remarkable agreement with most recent experimental data [28]. Note that for the inverse reaction the relevance of the p wave contributions has been pointed out also in [5–8].

Two fragment photodisintegration of the three-nucleon bound states, thus, provides a sensitive tool for testing the underlying two-nucleon potentials. A repetition of the corresponding low-energy measurements with much higher accuracy is strongly suggested by this observation.

ACKNOWLEDGMENTS

This work was supported by the Deutsche Forschungsgemeinschaft under Grant No. Sa 327/23-1.

TABLES

TABLE I. Parameters for the Yamaguchi-Potential. The numbers in parenthesis are taken from [2].

		Binding				
		Strength	Inverse range	Scattering length	Effective range	energy
Interaction		λ (fm $^{-3}$)	β (fm $^{-1}$)	a (fm)	r_0 (fm)	(MeV)
$n-p$ triplet	I	0.3815	1.406	5.433	1.761	-2.203
				(5.423)	(1.761)	(-2.225)
$n-p$ singlet	II	0.220	1.15	5.806	2.088	-2.082
				(5.68)	(2.09)	(-2.225)
$n-p$ singlet	I	0.1445	1.153	-23.196	2.732	
				(-23.715)	(2.74)	
$p-p$ singlet	II	0.148	1.15	-42.217	2.680	
				(-21.25)	(2.74)	
$n-n$ singlet		0.1534	1.223	-7.853	2.794	
				(-7.823)	(2.794)	
$n-n$ singlet		0.1323	1.130	-16.851	2.841	
				(-17.0)	(2.84)	
$n-p$ triplet	III	-0.220	1.14525	5.666	2.081	2.226
$n-n$ singlet	III	-0.148	1.16225	-22.998	2.710	

TABLE II. Parameters for the Malfliet-Tjon-Potential.

	σ	λ_σ^A [fm $^{-2}$]	λ_σ^R [fm $^{-2}$]	r_σ^A [fm]	r_σ^R [fm]	
s		-19.5719				
	d	-23.8775	109.605	0.643087	0.321543	

TABLE III. Triton Binding energies obtained with the Yamaguchi-Potentials. The numbers in parenthesis are taken from [2].

Wave function	Interaction set	Binding energy (MeV)
Symmetric Tabakin	Average of $n - p$	9.72
	triplet and singlet	(9.33)
	sets II	
Tabakin	$n - p$ triplet and singlet sets II	10.11 (10.1)
Charge dependent	$n - p$ triplet I	10.34
^3H	$n - p$ singlet I	(10.34)
	$n - n$ singlet	
Charge dependent	$n - p$ triplet	8.49
	$\lambda = 0.3608 \text{ fm}^{-3}$	(8.49)
^3H	$n - p$ singlet I	
(adjusted)	$n - n$ singlet	
Charge dependent	$n - p$ triplet I	7.72
	$\lambda = 0.3589 \text{ fm}^{-3}$	(7.72)
^3He	$n - p$ singlet I	
(adjusted)	$p - p$ singlet	
^3H	$n - p$ singlet III	9.968
(present)	$n - n$ singlet III	

REFERENCES

- [1] I. M. Barbour and A. C. Phillips, Phys. Rev. C **1**, 165 (1970).
- [2] B. F. Gibson and D. R. Lehman, Phys. Rev. C **11**, 29 (1975).
- [3] A. C. Fonseca and D. R. Lehman, Phys. Lett. **B 267**, 159 (1991).
- [4] A. C. Fonseca and D. R. Lehman, in *Few-Body Systems, Suppl. 6*, 279 (1992), Phys. Rev. C **48**.
- [5] A. C. Fonseca and D. R. Lehman, Phys. Rev. C **48**, R503 (1993).
- [6] S. Ishikawa, in *Few-Body Problems in Physics, Suppl. 6*, 295 (1992).
- [7] A. C. Fonseca and D. R. Lehman, in *Proceedings of the 14th International IUPAP Conference on Few-Body Problems in Physics, Williamsburg, VA 1994*, Ed. Franz Gross (AIP, New York, 1995).
- [8] G. J. Schmid, R. M. Chastel, H. R. Weller, D. R. Tilley, A. C. Fonseca, and D. R. Lehman, Phys. Rev. C **53**, 35 (1996).
- [9] E. O. Alt, P. Grassberger, and W. Sandhas, Nucl. Phys. **B2**, 167 (1967).
- [10] W. Sandhas, in *Few-Body Systems, Suppl. 1*, 64 (1986).
- [11] E. A. Bartrnik, H. Haberzettl, and W. Sandhas, Phys. Rev. C **34**, 1520 (1986).
- [12] Th. Januschke, T. Frank, W. Sandhas, and H. Haberzettl, Phys. Rev. C **47**, 1401 (1993).
- [13] D. J. Ernst, C. M. Shakin, and R. M. Thaler, Phys. Rev. C **8**, 46 (1973), Phys. Rev. C **9**, 1780 (1974).
- [14] J. Haidenbauer and W. Plessas, Phys. Rev. C **30**, 1822 (1984).
- [15] J. Haidenbauer, Y. Koike, and W. Plessas, Phys. Rev. C **30**, 1822 (1984).
- [16] J. Haidenbauer private communications.

[17] E. A. Bartnik, H. H. T. Januschke, U. Kerwath, and W. Sandhas, Phys. Rev. C **36**, 1678 (1987).

[18] A. J. F. Siegert, Phys. Rev. **52**, 787 (1937).

[19] M. M. Gianini and G. Ricco, *Photoreactions above the Giant Dipole Resonances* (Springer, New York, 1985).

[20] H. Arenhövel and M. Sanzone, *Few-Body Systems Suppl. 3* (1991) .

[21] Y. Yamaguchi, Phys. Rev. **95**, 1628 (1954), Phys. Rev. **95**, 1635 (1954).

[22] M. Lacombe, B. Loiseau, J. M. Richard, and R. Vinh Mau, Phys. Rev. C **21**, 861 (1980).

[23] R. Machleidt, K. Holinde, and Ch. Elster, Phys. Rep. **149**, 1 (1987).

[24] R. A. Malfliet and J. A. Tjon, Ann. Phys. **61**, 425 (1970).

[25] G. Ellerkmann, W. Sandhas, S. A. Sofianos, and H. Fiedeldey, Phys. Rev. C **53**, 2638 (1996).

[26] R. Kosiek, D. Müller, and R. Pfeiffer, Phys. Lett. **21**, 199 (1966).

[27] D. D. Faul, B. L. Berman, P. Meyer, and D. L. Olson, Phys. Rev. Lett. **44**, 129 (1980).

[28] D. M. Skopik, D. H. Beck, J. Asai, and J. J. Murphy II, Phys. Rev. C **24**, 1791 (1981).

FIGURES

FIG. 1. Triton photodisintegration cross section for the Yamaguchi potential compared with [2].

FIG. 2. Same as Fig. 1 but for ${}^3\text{He}$.

FIG. 3. Triton photodisintegration cross sections for the Yamaguchi, Malfliet-Tjon, Paris and Bonn B potentials.

FIG. 4. Triton photodisintegration cross sections for the Paris potential ($j \leq 1^+$) with and without Siegert's theorem.

FIG. 5. Cross sections for the Paris potential ($j \leq 1^+$) compared with the data from Refs. [23-25].

FIG. 6. Same as Fig. 5 for the Bonn B potential.

FIG. 7. Cross sections for the Paris potential with incorporation of the p waves ($j \leq 1$) compared with the data from Refs. [23-25].

FIG. 8. Same as Fig. 7 for the Bonn B potential.

Fig.1

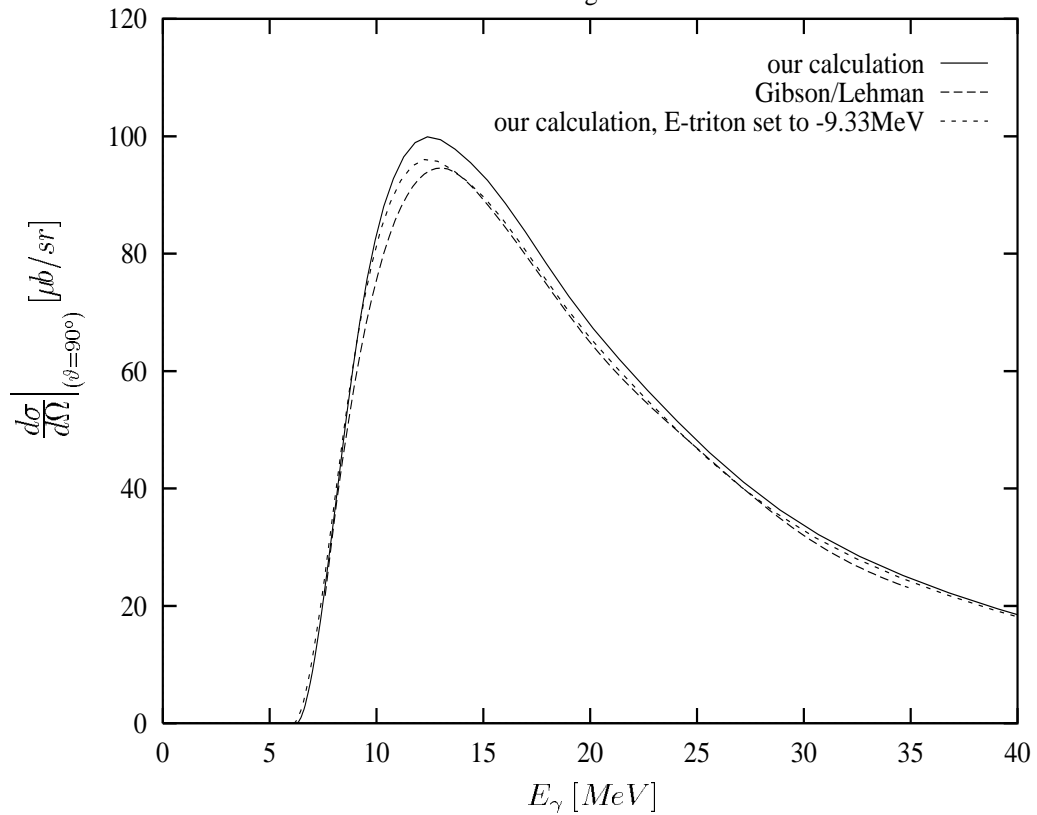


Fig.2

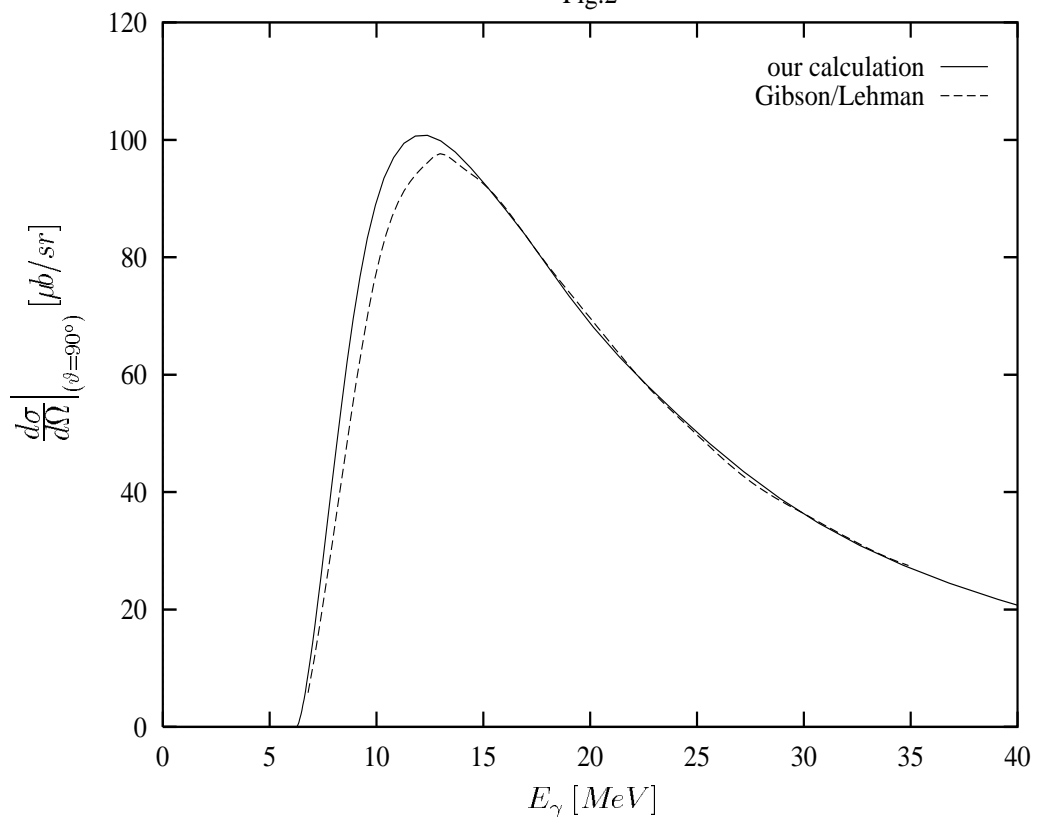


Fig. 3

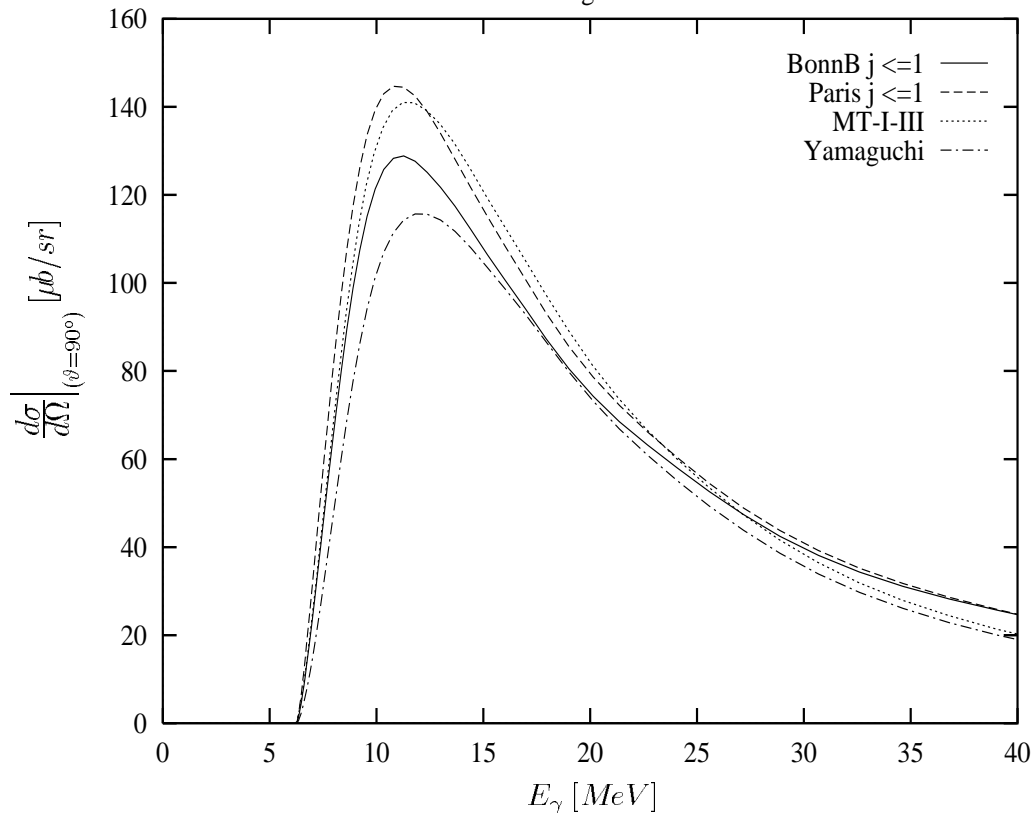


Fig.4

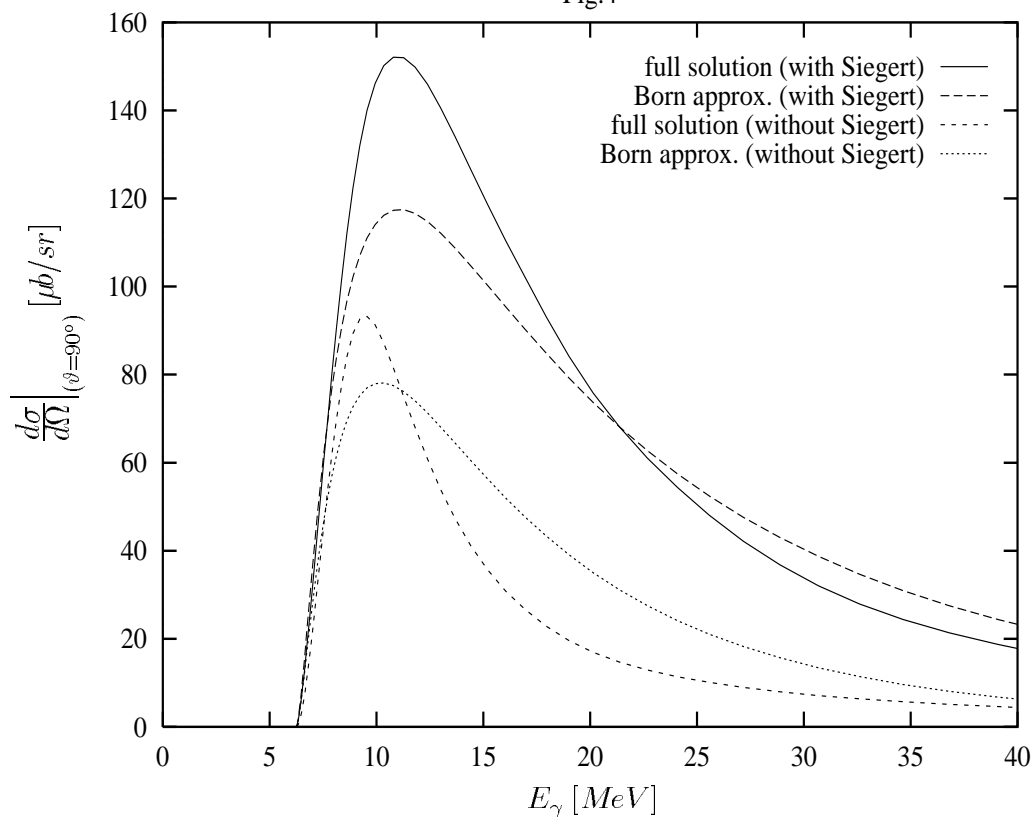


Fig.5

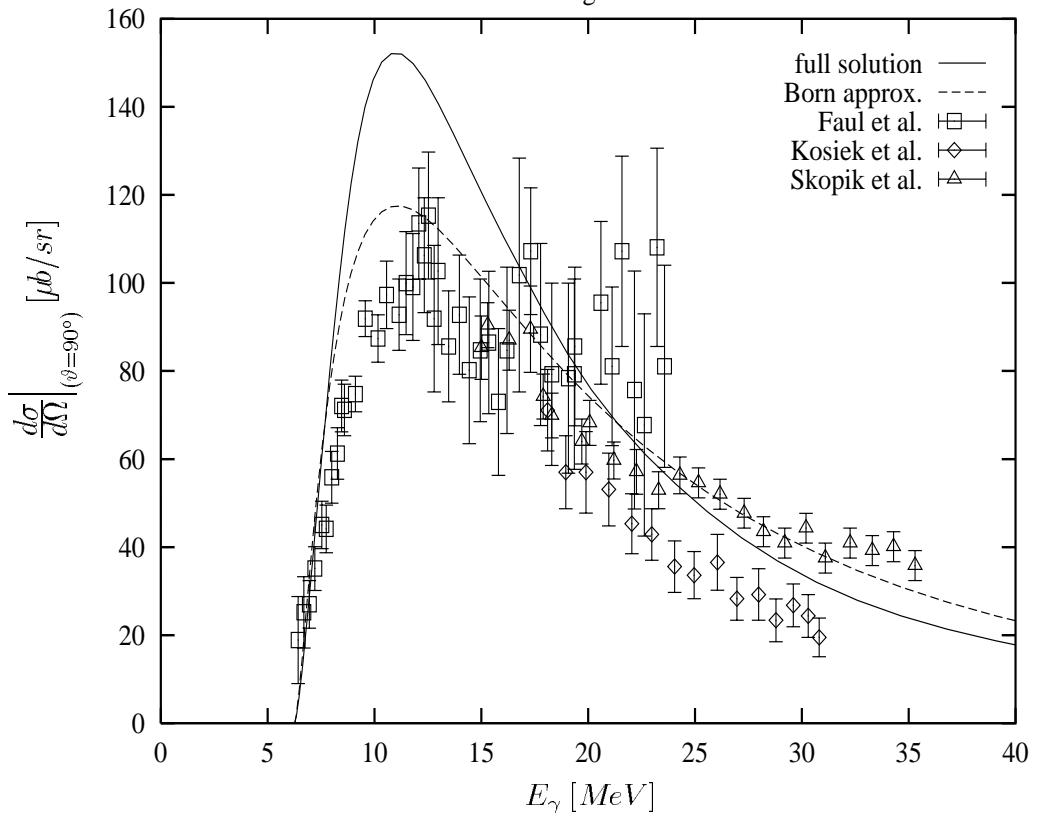


Fig. 6

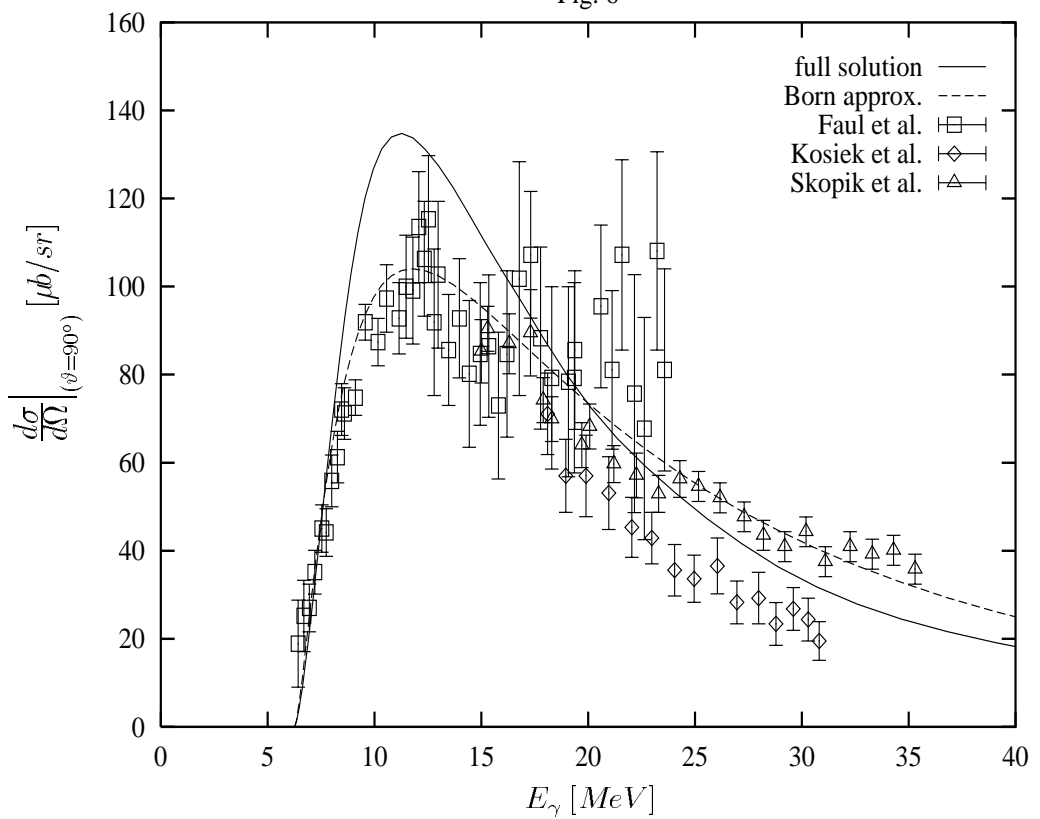


Fig. 7

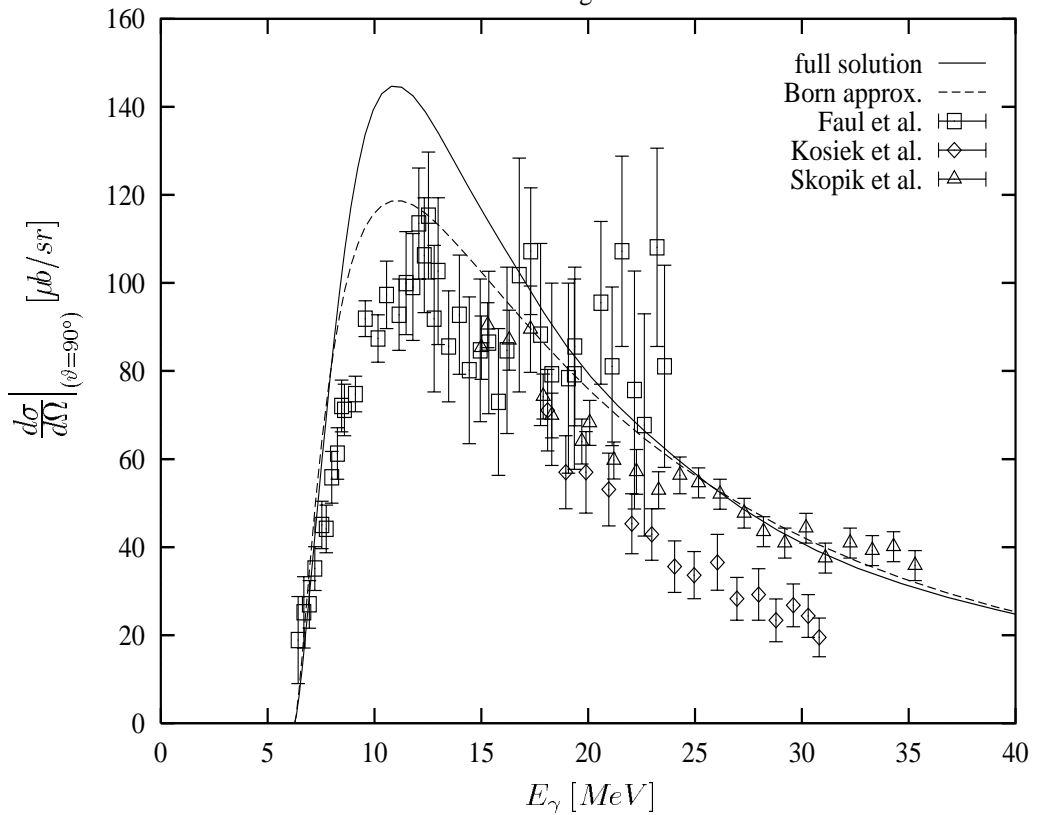


Fig. 8

